VESSELNESS ESTIMATION THROUGH HIGHER-ORDER ORIENTATION TENSORS

Rodrigo Moreno and Örjan Smedby

School of Technology and Health
KTH Royal Institute of Technology
{rodrigo.moreno,orjan.smedby}@sth.kth.se

ABSTRACT

We recently proposed a method for estimating vesselness based on detection of ring patterns in the local distribution of the gradient. This method has a better performance than other state-of-the-art algorithms. However, the original implementation of the method makes use of the spherical harmonics transform locally, which is time consuming. In this paper we propose an equivalent formulation of the method based on higher-order tensors. A linear mapping between the spherical harmonics transform and higher-order orientation tensors is used in order to reduce the complexity of the method. With the new implementation, the analysis of computed tomography angiography data can be performed 2.6 times faster compared with the original implementation.

***Index Terms*—** Vesselness, Spherical harmonics, Higher-order tensors

1. INTRODUCTION

Vesselness methods aim at extracting structures with tubular shape in medical images. We recently proposed a vesselness method that is based on the analysis of the filtered local orientation distribution of the gradient (LODG) in the spherical harmonics domain [1]. Despite the fact the method yields better results than previously proposed methods, its main drawback is its computational cost. The most intensive computational procedure in our method is to perform the spherical harmonics expansion of the LODG. Performing such an expansion in a more efficient way can make it applicable in scenarios where efficiency is an issue.

Thus, the main aim of this paper is to propose an alternative way to get the spherical harmonics decomposition, also known as spherical harmonics transform (SHT), which is based on higher-order orientation tensors. Related approaches have been proposed in the diffusion imaging research community (e.g., [2, 3]). In fact, the present work can be seen as a generalization of these approaches that can be used for any orientation function, not only for those with antipodal symmetry used in diffusion imaging.

This research has partially been funded by the Swedish Research Council (VR), grants no. 2014-6153 and 2012-3512, and the Swedish Heart-Lung Foundation (HLF), grant no. 2011-0376.

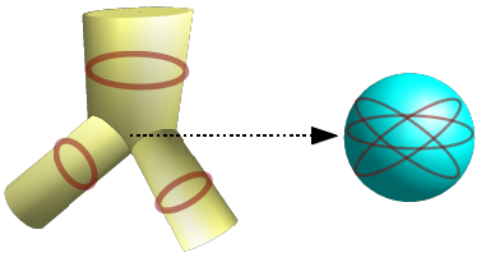

Fig. 1. Left: a Y-bifurcation and the orientation of the gradients (in red). Right: the LODG for the center of the bifurcation with three ring patterns, one per branch. Vessels can be enhanced by detecting ring patterns in the LODG.

The paper is organized as follows. Section 2 summarizes the method proposed in [1]. Section 3 describe the linear relationship between the SHT and higher-order orientation tensors. Section 4 describes some implementation issues. Section 5 compares the original and the proposed implementation. Finally 6 discusses the results and makes some concluding remarks.

2. GRADIENT-BASED VESSELNESS

The main observation in [1] is that the LODG at vessel structures exhibit ring-like patterns as shown in Fig. 1.

The method follows three stages per voxel: creation of the LODGs, feature extraction of the LODGs and combination of features. In the first stage, gradients of the neighbors not pointing to the studied voxel are discarded, as they can lead to errors in the analysis. Then, the LODG is created with the surviving gradient vectors. In the second stage, different features are extracted from the LODG in the spherical harmonics domain as follows. First, the SHT of the LODG is computed. Second "evenness" E, "uniformness" U and "structuredness" S measurements are computed from the power spectrum of the LODG in the spherical harmonics domain. Finally, modified measures of evenness and uniformness, $E_{1/2}$ and $U_{1/2}$, are estimated using the same procedure applied to the LODG

where half of the distribution is set to zero. In the final stage, E, U, S, $E_{1/2}$ and $U_{1/2}$ are combined into a single vesselness measure at the studied voxel, in which LODGs with ring-like patterns will have a higher value, making easier the discrimination between vessel and non-vessel regions. More details can be found in the original paper. As already mentioned, the most computationally intensive step of the method is the computation of the SHT of the LODG.

3. RELATIONSHIP BETWEEN SPHERICAL HARMONICS AND HIGHER-ORDER TENSORS

In this section, we describe the proposed method for computing the SHT using just two higher-order orientation tensors. In spherical coordinates, spherical harmonics of degree ℓ and order m can be written as:

$$Y_\ell^m = \sqrt{\frac{(2\ell+1)}{4\pi}\frac{(\ell-m)!}{(\ell+m)!}}\, P_\ell^m(\cos\theta)\, e^{im\varphi}, \qquad (1)$$

where P_ℓ^m are the associated Legendre polynomials, and θ and φ are the collatitude and azimuth angles respectively. Since spherical harmonics constitute a orthonormal basis in the surface of the unitary sphere S^2, a function f such that $\int_{S^2} f d\Omega = 1$ with $d\Omega$ being the surface element of S^2 can be expanded in terms of spherical harmonics as:

$$f = \sum_{\ell=0}^{\infty}\sum_{m=-\ell}^{\ell} A_\ell^m Y_\ell^m, \qquad (2)$$

where A_ℓ^m are computed as:

$$A_\ell^m = \int_{S^2} f\, \overline{Y}_\ell^m\, d\Omega \qquad (3)$$

with $\overline{Y}_\ell^m$ being the complex conjugate of Y_ℓ^m. An important property of such a decomposition, also known as SHT, is that $A_\ell^m = 0$ for ℓ odd for functions with antipodal symmetry, and $A_\ell^m = 0$ for ℓ even for functions with antipodal skew symmetry [4, 5].

In [1], we used the aformentioned expansion using spherical coordinates. However, such an expansion can also be performed in cartesian coordinates by using the definition of spherical harmonics with cartesian coordinates x, y and z, which is given by:

$$Y_\ell^m = (-1)^m 2^{-\ell}\sqrt{\frac{2\ell+1}{4\pi}\frac{(\ell-m)!}{(\ell+m)!}}\,\Pi_\ell^m\,(P_m + iQ_m) \quad (4)$$

where:

$$P_m = ((x+iy)^m + (x-iy)^m)/2 \qquad (5)$$

$$Q_m = ((x+iy)^m - (x-iy)^m)/2i \qquad (6)$$

$$\Pi_\ell^m = \sum_{k=0}^{t}(-1)^k\binom{\ell}{k}\binom{2(\ell-k)}{\ell}\frac{(\ell-2k)!}{(\ell-2k-m)!}z^{\ell-2k-m} \qquad (7)$$

with $t = \lfloor(\ell-m)/2\rfloor$.

The main consequence of (4) is that spherical harmonics can be represented by polynomials on x, y and z of degree equal to or lower than ℓ. An important property of these polynomials is that the monomials in (4) are of even degree for ℓ even and of odd degree for ℓ odd. This means that the degree of the ith monomial of Y_ℓ^m, d_i, is related to ℓ by the relationship $d_i = \ell - 2k_i$ with $k_i \geq 0$ and $d_i \geq 0$.

Since Y_ℓ^m is defined in S^2, the cartesian coordinates are related by $x^2+y^2+z^2 = 1$. Using this relationship, it is possible to express Y_ℓ^m by homogeneous polynomials of degree $L = \ell + 2K$ for any $K \geq 0$ by replacing the every monomial M_i of Y_ℓ^m by $M_i(x^2+y^2+z^2)^{K+k_i}$. This simple procedure leads to an equivalent polynomial where all monomials are of order L. As an example, Y_2^0 can be expressed equivalently through homogeneous polynomials of degree 2, 4 or 6 as:

$$\begin{aligned} 4\sqrt{\frac{\pi}{5}}Y_2^0 &= -x^2 - y^2 + 2z^2 \\ &= -x^4 - 2x^2y^2 + x^2z^2 - y^4 + y^2z^2 + 2z^2 \\ &= -x^6 - 3x^4y^2 - 3x^2y^4 + 3x^2z^4 - y^6 + \\ &\quad 3y^2z^4 + 2z^6. \end{aligned}$$

Therefore, Y_ℓ^m can be written as a linear combination of the monomial basis of homogeneous polynomials of degree $L = \ell + 2K$ on x, y and z. Hence, $Y_\ell^m = \langle C_L(\ell,m), B_L\rangle$ where $C_L(l,m)$ is a vector of complex constants and $B_L = (x^L, x^{L-1}y, x^{L-1}z, x^{L-2}y^2, x^{L-2}yz, x^{L-2}z^2, ..., z^L)^T$ is the monomial basis.

Let us consider a sampled function in S^2, which without loss of generality can be written as:

$$f(\vec{n}) = \sum_{j=1}^{N} f_j \delta(\vec{n_j} - \vec{n}), \qquad (8)$$

where δ is the impulse function, $\vec{n}$ and $\vec{n_j}$ are unitary vectors and f_j is the value of the function at $\vec{n_j}$. Notice that the LODGs can be modeled in this way, with f_i being the weighted norm of the gradient and n_j the normalized gradients that appear in a specific neighborhood. By applying (3), we get:

$$A_\ell^m = \sum_{j=1}^{N} f_j \overline{Y}_\ell^m(\vec{n_j}) = \overline{C}_L(\ell,m)\sum_{j=1}^{N} f_j B_L(\vec{n_j}). \qquad (9)$$

Observe that, since $Y_\ell^{-m} = (-1)^m\overline{Y}_\ell^m$, then $A_\ell^{-m} = (-1)^m\overline{A}_\ell^m$. It is not difficult to show that the summation on the right hand side of (9) corresponds to the entries of the so-called orientation tensor of order L, which is given by:

$$D_L = \sum_{j=1}^{N} f_j \vec{n_j}^{\otimes L}, \qquad (10)$$

where $\vec{n_j}^{\otimes L}$ is the Lth-power outer product of $\vec{n_j}$ [4].

The main result of (9) is that, since $C_L(\ell, m)$ is constant, there is a linear connection between the SHT and higher-order orientation tensors of order $L = \ell + 2K$ for any $K \geq 0$. It is important to highlight that the representation in (9) is compact in the sense that just two orientation tensors are necessary to compute all A_ℓ^m for any $\ell \leq L$, namely D_L and D_{L-1}, which are used for computing A_ℓ^m of even and odd degrees respectively.

Let D_L^* and D_{L-1}^* be vectors with the independent entries of D_L and D_{L-1} respectively. Then, (9) can be rewritten in a more compact way as:

$$\left(A_0^0, A_2^0, A_2^1, ..., A_L^L\right)^T = \overline{C}_L D_L^* \quad (11)$$

$$\left(A_1^0, A_1^1, A_3^0, ..., A_{L-1}^{L-1}\right)^T = \overline{C}_{L-1} D_{L-1}^*. \quad (12)$$

As already mentioned, A_ℓ^{-m} can be computed from A_ℓ^m. Thus, only the coefficients with $m \geq 0$ are necessary to be computed. Consequently, $\overline{C}_L$ and $\overline{C}_{L-1}$ are non-squared constant matrices of sizes $(L+2)^2/4 \times (L+1)(L+2)/2$ and $(L^2/4 + L/2) \times (L^2/2 + L/2)$ respectively. For example, the sizes of $\overline{C}_6$ and $\overline{C}_5$ are 16×28 and 12×21 respectively. From this, it can be said that the spherical harmonics expansion is a more compact representation of functions in S^2 than higher-order tensors of order L and $L-1$. This is actually an expected result, since the procedure for homogenizing of polynomials of Y_ℓ^m described above creates extra entries when higher degrees are applied.

In summary, there are mainly two ways to compute the SHT of a function in S^2: either through (3) or (9). Both approaches have advantages and drawbacks. On the one hand, (9) is more convenient when the number of sampling points N in (8) and L are relatively small, since the computation of orientation tensors will be inexpensive both in time and memory consumption. If these conditions are not given, (3) is more appropriate, especially considering that efficient implementations are already available [6]. Depending on the method, the function has to be approximated using a mesh or a grid in this case. Using a coarse mesh or grid can speed up the computations but at a cost of an increased inaccuracy. This is not an issue for the higher-order tensor-based implementation.

4. IMPLEMENTATION

In the specific case of the method in [1], L can be limited to 6, which is enough for resolving Y-branches in the vessels. Algorithm 1 summarizes the process for estimating vesselness with higher-order orientation tensors, where G is a Gaussian decaying function with parameter σ.

The method requires to precompute $(\nabla I/||\nabla I||)^{\otimes 6}$ and $(\nabla I/||\nabla I||)^{\otimes 5}$, which corresponds to 28 + 21 = 49 features per voxel. Observe that the loop mainly consists of simple arithmetic operations and, since the computations are performed per voxel, it is easy to parallelize.

Algorithm 1 Vesselness Estimation

Precompute per voxel $g_6 = (\nabla I/||\nabla I||)^{\otimes 6}$
Precompute per voxel $g_5 = (\nabla I/||\nabla I||)^{\otimes 5}$
for all $\vec{p}$ **do** ▷ $\vec{p}$ is a voxel in the image
  Select neighbors $\vec{q}$ of $\vec{p}$ such that $\langle \nabla I_{\vec{q}}, \vec{q} - \vec{p} \rangle \leq 0$
  Compute $f_{\vec{q}} = G(||\vec{p} - \vec{q}||)\, ||\nabla I_{\vec{q}}||$
  Compute $D_6(\vec{p}) = \sum_{\vec{q}} f_{\vec{q}}\, g_6(\vec{q})$
  Compute $D_5(\vec{p}) = \sum_{\vec{q}} f_{\vec{q}}\, g_5(\vec{q})$
  Compute $A_\ell^m(\vec{p})$ using (11) and (12)
  Compute the autocorrelation power spectrum $P_\ell(\vec{p})$
  Compute $E(\vec{p})$, $U(\vec{p})$ and $S(\vec{p})$
  Select neighbors $q_{1/2}$ from $\vec{q}$ such that $\nabla I_{\vec{q}}(3) \geq 0$
  Do 6:10 for $\vec{q}_{1/2}$ to compute $E_{1/2}(\vec{p})$ and $U_{1/2}(\vec{p})$
  Compute vesselness as described in [1]
end for

5. RESULTS

The vesselness method was applied to one of the computed tomography angiography (CTA) datasets provided by the coronary artery stenoses detection and quantification and lumen segmentation in CTA images challenge [7] [1] with the original, which uses the efficient method proposed in [8], and the proposed implementation. The image was resampled for having an isotropic resolution of 0.4mm. The methods were coded in MATLAB and run in a workstation with 6 Intel Xeon CPUs at 2.4GHz and 32GB of RAM. The method in [8] has been applied using a sampling grid with a resolution of 1 degree.

Figure 2 shows the evolution of the execution time for both implementations for different values of σ of the Gaussian function. The size of the neighborhood is mainly determined by this variable. As shown, the new implementation is more sensitive to the size of the neighborhood. However, it is also more efficient for small values of σ. Notice that the method requires a single value of σ which is related to the maximum diameter of the vessels. Since the maximum diameter of the coronary arteries is approximately 4.5 mm [9], a σ of 0.75 mm should be appropriate for enhancing most of the vessels with the proposed method. This means that for this specific application, the proposed implementation is 2.6 times faster than the original one.

The two implementations are expected to yield similar but not exactly the same result. The differences between the two methods come from the fact that the original implementation requires the LODGs to be fit into a prescribed grid. The implementation with higher-order tensors is in that sense more accurate. Table 1 shows the root-mean-squared error (RMSE) between the two implementations with different σ. Considering that the vesselness values range between 0 and 1, the observed RMSE is very small. This means that, in practice, both methods yield almost the same result.

[1] We thank Hortense Kirişli, Theo van Walsum and Wiro Niessen for providing this dataset.

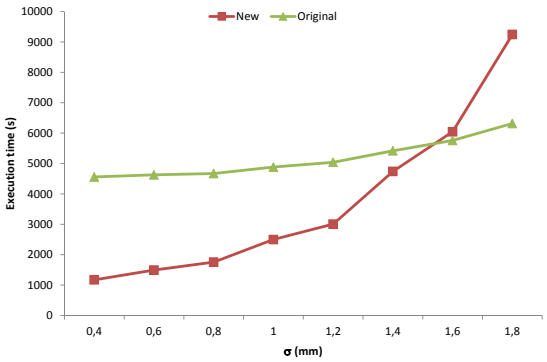

Fig. 2. Evolution of the execution time with the size of the neighborhood for estimating vesselness on the CTA dataset number 5 in [7] using the original and the proposed implementation, which is based on higher-order tensors.

Table 1. RMSE between the original and the proposed implementation for estimating vesselness on the CTA dataset number 5.

$\sigma(mm)$	0.4	0.6	0.8	1.0	1.2
RMSE	0.0005	0.0007	0.0012	0.0017	0.0020

6. DISCUSSION

We proposed a new implementation of the method in [1] based on higher-order orientation tensors that yields faster results in CTA data. Although efficient implementations of the spherical harmonics transform are available (e.g. [6]) they require discretizations into grids or meshes that can lead to inaccuracies, which is not an issue for the proposed implementation. In general, such methods are preferred when L and the number of sampling data N are large. This is usually not the case for estimating vesselness, since the analysis is performed in relatively small neighborhoods. From the results, the proposed implementation is 2.6 faster than the original one for enhancing the coronary arteries in CTA data. Further efficiency improvements are expected by performing the computations in the GPU. Regardless of σ, the new implementation requires extra memory for storing 49 precomputed features per voxel. This can be reduced by preselecting potential voxels that must be analyzed (see [1]).

It is worthwhile to point out that the proposed generalization of the relationship between spherical harmonics and higher-order tensors is applicable to other applications where the spherical harmonics transform is required. For example, the vesselness method proposed in [10], which is also based on spherical harmonics, could also benefit of the proposed method. Our current research includes a more exhaustive evaluation with more datasets.

7. REFERENCES

[1] R. Moreno and Ö. Smedby, "Gradient-based enhancement of tubular structures in medical images," *Med Image Anal*, vol. 26, no. 1, pp. 19–29, 2015.

[2] M. Descoteaux, E. Angelino, S. Fitzgibbons, and R. Deriche, "Apparent diffusion coefficients from high angular resolution diffusion imaging: Estimation and applications," *Mag Reson Med*, vol. 56, no. 2, pp. 395–410, 2006.

[3] E. Özarslan and T. H. Mareci, "Generalized diffusion tensor imaging and analytical relationships between diffusion tensor imaging and high angular resolution diffusion imaging," *Magn Res Med*, vol. 50, no. 5, pp. 955–965, 2003.

[4] M. Moakher and P. J. Basser, *In: Visualization and Processing of Higher Order Descriptors for Multi-Valued Data, I. Hotz and T. Schultz (eds)*, chapter Fiber Orientation Distribution Functions and Orientation Tensors for Different Material Symmetries, pp. 37–71, Springer, 2015.

[5] K. Kanatani, "Distribution of directional data and fabric tensors," *Int J Eng Sci*, vol. 22, no. 2, pp. 149–164, 1984.

[6] N. Schaeffer, "Efficient spherical harmonic transforms aimed at pseudospectral numerical simulations," *Geochem, Geophys, Geosyst*, vol. 14, no. 3, pp. 751–758, 2013.

[7] H. A. Kirişli et al., "Standardized evaluation framework for evaluating coronary artery stenosis detection, stenosis quantification and lumen segmentation algorithms in computed tomography angiography," *Med Image Anal*, vol. 17, no. 8, pp. 859 – 876, 2013.

[8] J. R. Driscoll and D. M. Healy, "Computing Fourier transforms and convolutions on the 2-sphere," *Adv Appl Math*, vol. 15, no. 2, pp. 202–250, 1994.

[9] J. T. Dodge, B G. Brown, E. L. Bolson, and H. T. Dodge, "Lumen diameter of normal human coronary arteries. influence of age, sex, anatomic variation, and left ventricular hypertrophy or dilation.," *Circ*, vol. 86, no. 1, pp. 232–246, 1992.

[10] D. Rivest-Hénault and M. Cheriet, "3-D curvilinear structure detection filter via structure-ball analysis," *IEEE Trans. Image Process.*, vol. 22, no. 7, pp. 2849–2863, 2013.